

Using wind tunnel tests to study pressure distributions around a bluff body: the case of a circular cylinder

Josué Njock Libii

Indiana University-Purdue University Fort Wayne
Fort Wayne, Indiana, United States of America

ABSTRACT: Hands-on exercises were designed and tested in a subsonic wind tunnel to study pressure distributions around a circular cylinder in cross flow. They allowed students to collect their own data and use them to examine how the pressure on the surface of the cylinder changes with two different variables: the location of a given point along the circumference of the middle cross section of the cylinder and the magnitude of the Reynolds number of the flow. Plotted data produced curves very similar to those in the research literature. Detailed examination of results demonstrated how viscous flow behaviour in the upstream half of the cylinder differed from that on its downstream half. The influence of the magnitude of the Reynolds number on the ability of the viscous flow to recover pressure on the downstream side of the cylinder was demonstrated.

INTRODUCTION

Many exercises can be designed and tested in the fluid mechanics laboratory to study pressure distributions around bluff bodies in the wind tunnel. While many bluff objects, such as cylinders, spheres, miniature vehicles and buildings, can be studied, circular cylinders are, by far, the easiest [1]. This is because cross flow over a very long cylinder can be reasonably approximated as being two dimensional.

A body is said to be streamlined, if fluid flow over it essentially follows the contours of the body. Here, the geometric shape of the body defines the geometric shape of the streamlines adjacent to the body. Airplane wings are examples of streamlined bodies. A body that is not streamlined is said to be bluff. Therefore, fluid flow over a bluff body follows the contours of that body only part way, or not at all. Here, then, the shape of the body does not define the shape of the streamlines adjacent to it. Cylinders, spheres, buildings, ships, trees, and animals, are examples of bluff bodies [2]. When flow that was near the surface ceases to follow the contour of the body, flow is said to have separated from that body. The point at which separation is first observed is called the point of separation [3]. An example of flow separation over the front of a car is shown below in Figure 1.

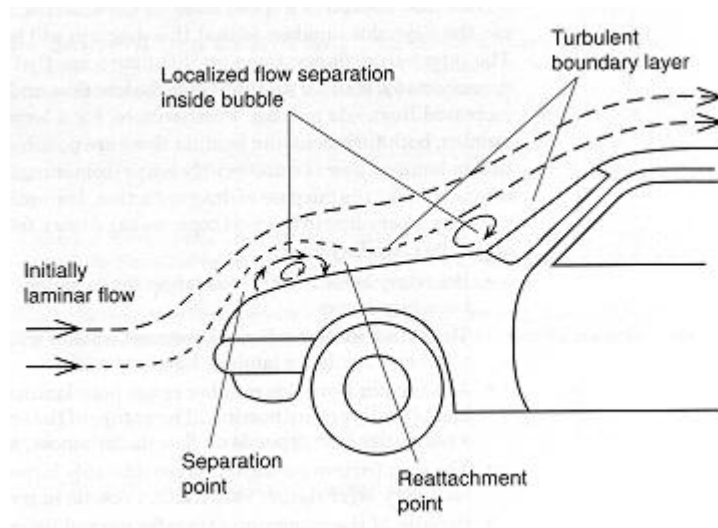


Figure 1: Illustrated flow separation over the front of a moving automobile [2].

The study of flows over cylinders allows students to determine how the pressure changes with two different variables, which are the location of a point along the circumference of the cylinder and the magnitude of the Reynolds number of the flow [4]. It also gives them the opportunity to have practical experience with the concepts of pressure drag, flow separation and viscous wakes through hands-on learning [1].

The variation of pressure over a circular cylinder is typically presented in fluid mechanics papers and textbooks as a graph [4-6]. The main purposes of that graph are to demonstrate and quantify the differences between the behaviour of ideal flows, which are assumed frictionless, and that of real flows, which always have friction. Three ways that are used to demonstrate these differences are the patterns of flow streamlines over the body [3], the creation, generation, and shedding of vorticity behind submerged objects [3], and the variation of pressure around the circumference of the cylinder [4-6]. Whereas the first two methods require sophisticated means to visualise the flow, the last one is quite easy to use, provided that one has access to a wind tunnel and some pressure probes. The purpose of this article is to illustrate the variation of pressure around the circumference of the cylinder by using data collected by undergraduate students in a subsonic wind tunnel.

The remainder of the article is organised in the following manner: First D'Alembert's paradox is stated and proved in the case of a circular cylinder; this paradox is used as a stepping stone to discuss pressure distributions around a cylinder in the cross flow of a viscous fluid. Next, the concept of the pressure coefficient is introduced and its use in the literature is illustrated and explained. Then, experiments carried out by students in the wind tunnel are described; their results are presented and compared to the literature. Finally, the results are interpreted to elucidate the effects of the magnitude of the Reynolds number on pressure distributions around a circular cylinder.

D'ALEMBERT'S PARADOX APPLIED TO A CIRCULAR CYLINDER

D'Alembert's paradox applied to a cylinder states that the net pressure drag exerted on a circular cylinder that moves in an inviscid fluid of large extent is identically zero. This result is proved below.

Consider the steady flow of a frictionless and incompressible fluid from left to right over a stationary circular cylinder of radius $r = a$. If the flow is horizontal and uniform at infinity with magnitude U and pressure P_∞ there, then, its velocity V , in the vicinity of the cylinder is given in cylindrical coordinates (r, θ) by:

$$\vec{V} = U \left[\left(1 - \frac{a^2}{r^2} \right) \cos \theta \right] \vec{e}_r - U \left[\left(1 + \frac{a^2}{r^2} \right) \sin \theta \right] \vec{e}_\theta, \quad (1)$$

where \vec{e}_r and \vec{e}_θ are unit vectors in the r - and θ -directions, respectively. From Eq. (1), the magnitude of the velocity at any point is given by:

$$V = U \left[1 + \left(\frac{a^2}{r^2} \right)^2 - 2 \left(\frac{a^2}{r^2} \right) \cos 2\theta \right]^{1/2}. \quad (2)$$

On the surface of the cylinder, where $r = a$, the magnitude given in Eq. (2) becomes:

$$V = 2U \sin \theta$$

The pressure, p_c , at a point of coordinates (a, θ) on the surface of the cylinder is found by using Bernoulli's equation along the streamline through that point. It is given by:

$$p_c = p_\infty + \frac{1}{2} \rho U^2 (1 - 4 \sin^2 \theta). \quad (3)$$

Since this flow has no friction, the total drag is due to pressure and it can be obtained by evaluating the following integral over the surface of the cylinder:

$$F_D = - \int_A p_c dA \cos \theta, \quad (4)$$

where p_c is given by Eq. (3), and dA is an element of surface area on the surface of the cylinder given by $dA = aLd\theta$, with L being the length of the cylinder. Evaluation of the integral in Eq. (4) around the circumference of the cylinder yields:

$$F_D = aL \left\{ \frac{4}{3} \rho U^2 \sin^3 \theta - \left(p_\infty + \frac{1}{2} \rho U^2 \right) \sin \theta \right\}_0^{2\pi}, \quad (5)$$

which is identically zero, thus, verifying D'Alembert's paradox. Historically, this result was called a paradox because real fluids, which are all viscous, do, in fact, exert drag forces on cylinders moving in them. This paradox is an excellent stepping stone to use to explain some features observed in the flow of viscous fluids around, or over immersed, objects of all kinds.

What happens in inviscid flow is that the pressure decreases continuously on the upstream half of the cylindrical surface in such a way that the drag force on that half is not zero. It can be verified that it is given by:

$$F_D \Big|_{\theta=-\pi/2}^{\theta=\pi/2} = 2aL \left[\frac{5\rho U^2}{6} - p_\infty \right].$$

However, pressure subsequently increases continuously on the downstream half of the cylinder in such a way that the drag force on it is the exact opposite of that developed over the upstream half. It can also be verified that it is given by:

$$F_D \Big|_{\theta=\pi/2}^{\theta=3\pi/2} = 2aL \left[p_\infty - \frac{5\rho U^2}{6} \right].$$

Thus, for the whole cylinder, then, the two opposing drag forces combine to give zero, demonstrating that all the pressure lost on the upstream half is recovered over the downstream half of the cylinder. This is what makes the net drag force over the whole cylinder zero. It was discovered that this paradox was made possible by the absence of friction [7]. Indeed, such total recovery of pressure on the downstream half of the cylinder does not occur in a real fluid, no matter how low its viscosity is.

THE PRESSURE COEFFICIENT

In order to compare the variation of pressure around a bluff body for a variety of flow conditions, it is conventional to use a dimensionless ratio called the pressure coefficient C_p , which compares the pressure on the surface of the cylinder, P_c , to that at infinity, P_∞ . It is defined by:

$$C_p \equiv \frac{P_c - P_\infty}{\frac{\rho U^2}{2}}. \quad (6)$$

When flow is inviscid, we combine Eq. (3) and Eq. (6) to get:

$$C_p = 1 - 4 \sin^2 \theta. \quad (7)$$

Unfortunately, a closed-form expression of C_p as a function of θ , similar to that shown in Eq. (7), cannot be obtained analytically when the fluid is viscous. This is because neither the pressure distribution nor the velocity is known at every point along the surface of the cylinder. However, one can measure the pressures at many points along a chosen cross section of the surface of the cylinder experimentally, compute C_p point by point using Eq. (6), and subsequently plot the results as a function of the position, θ , of each point where measurements were made. When such data have been plotted, the shape of the resulting curve and the magnitudes of the pressure coefficients at different points can be compared to those of the graph of Eq. (7), to determine the effects of viscosity and the Reynolds number.

The graph of pressure versus angular position on the circumference of the cylinder can be plotted using rectangular coordinates as shown in Figure 2, or using cylindrical polar coordinates, as shown in Figure 3. In Figure 2, only data for the top half of the cylinder were shown (from 0 to 180°). This is because flow is symmetrical about the horizontal diameter of the cylinder in inviscid, as well as viscous flows.

In Figure 3, however, the whole cross section of the cylinder is shown. Radial lines shown there indicate the magnitude of the pressure coefficient on the surface of the cylinder. The sign convention is as follows: radial lines shown outside the surface of the cylinder indicate negative pressure coefficients, whereas radial lines drawn inside the cylinder represent positive pressure coefficients. In Figure 2, as in Figure 3, it can be seen that, for inviscid flows, pressure recovery is complete on the downstream side of the cylinder. This is demonstrated by the existence of a vertical axis of

symmetry at $\theta = 90^\circ$. Such is not the case at all in viscous flows, even for a fluid such as air, which has a very low viscosity.

EFFECTS OF THE REYNOLDS NUMBER ON PRESSURE DISTRIBUTIONS

Students gathered data that would demonstrate the effect of the magnitude of the Reynolds number on the pressure distribution around the circular cylinder. The objective was to see whether or not they could generate results that were similar to those typically found in research papers and textbooks. Specifically, they were curious to see how close they could come to obtaining curves similar to those produced by Flachsbart [4] and Roshko [5], Figure 4.

A circular cylinder of diameter 1 in (2.54 cm) was tested in the test section of an open-circuit-Eiffel wind tunnel Model 402 B made by Engineering Laboratory Design, Inc., which has a velocity range of 3.0-48.7 m/s (10.0 – 160 fps) [11][12].

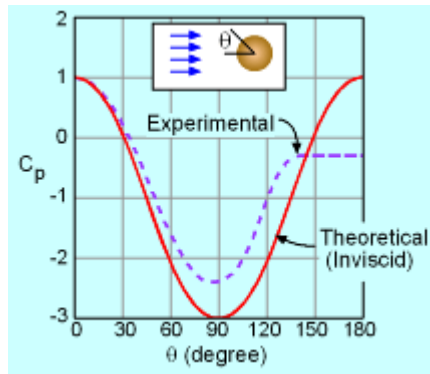


Figure 2: Comparison of pressure variations [8].

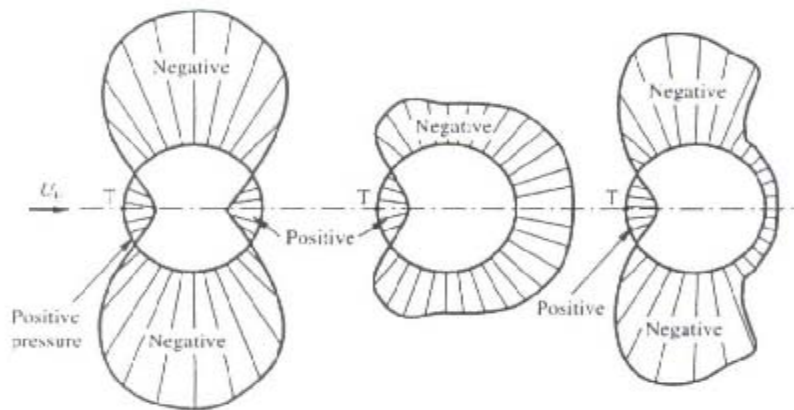


Figure 3: Comparison of pressure variations [9].

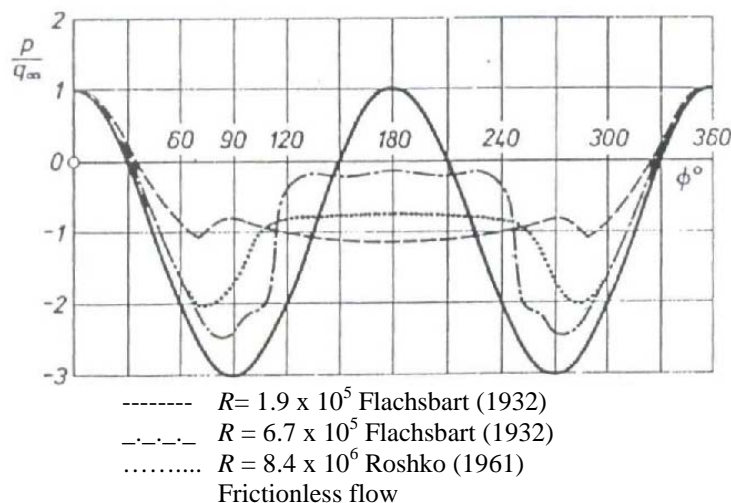


Figure 4: Standard curves for pressure distributions around a circular cylinder [4][5].

The cylinder was inserted in such a way that its longitudinal axis was perpendicular to the direction of the moving stream of air. This is known as cross flow. For a given setting of the wind speed in the tunnel, pressure probes were used to measure the pressure at selected points located all around the perimeter of the middle cross-section of the cylinder. Data were collected from 0° to 180° , using 10-degree increments around the upper surface of the cylinder. After a given run had been completed, the setting of the wind tunnel was changed to a new speed and the test was repeated. This process was continued until the maximum speed achievable by the wind tunnel was attained. This allowed for the cylinder to be tested at five different speeds: 15 mph, 30 mph, 60 mph, and 90 mph and 100 mph. The pressures that resulted from each speed setting were used to calculate the corresponding pressure coefficients using Eq.(6).

The resulting coefficients were then plotted as a function of the location of the points along the circumference of the cylinder as shown in Figure 5. That Figure also has the plot of Eq. (7), to make it possible to compare experimental data obtained using a viscous fluid to those obtained from the theory of inviscid flows. This resulted in a stack of curves that showed both the influence of the location of the point on the surface at which pressures were measured and the speed of air in the wind tunnel. Data obtained using speeds of 90 mph and 100 mph tests were not shown in Figure 5, because they were very close to those for 60 mph. Thus, they were eliminated to reduce crowding of the plots.

The Reynolds numbers corresponding to the tested wind speeds were 0.105×10^5 , 0.21×10^5 , 0.42×10^5 , 0.63×10^5 , and 0.76×10^5 , respectively. Each of these magnitudes is less than 5×10^5 , which is the critical value of the Reynolds number at which a boundary layer in external flow over a smooth cylinder transitions from laminar to turbulent. For cylinders that are not smooth, transition occurs earlier, at Reynolds numbers that are around 2×10^5 , Figure 6. Therefore, all the data collected using this setup were below the critical values above which the effects of turbulent boundary layers on the pressure distribution could be observed.

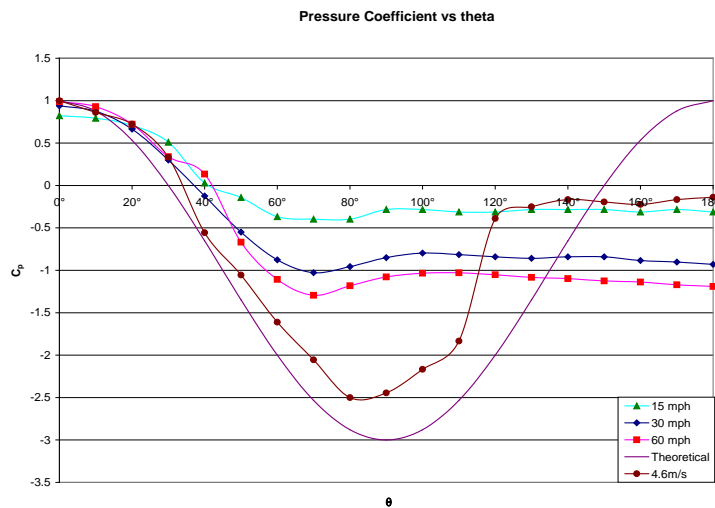


Figure 5: Plots of pressure distributions obtained in the lab.

To demonstrate this and give students a chance to compare their data with others for which the boundary layers were turbulent, several curves that are available in the literature were digitised and plotted next to the data students had collected. A sample stack of such plots is shown in Figure 5. The curve corresponding to a speed of 4.6 m/s had been obtained from an experiment that tested a cylinder of diameter $D = 1$ m in an airstream speed of 4.6 m/s. This corresponded to a Reynolds number of 2.84×10^5 [6]. It can be seen from Figure 5 that a flow with a Reynolds number of 2.84×10^5 helps the fluid recover the lost pressure much more effectively than the ones students had been able to test. This behaviour agrees with theory [3-7].

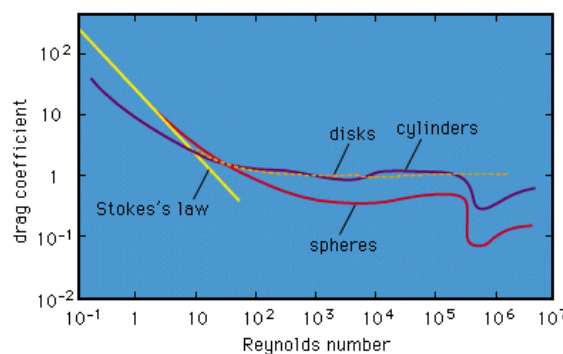


Figure 6: Drag coefficient for different objects.

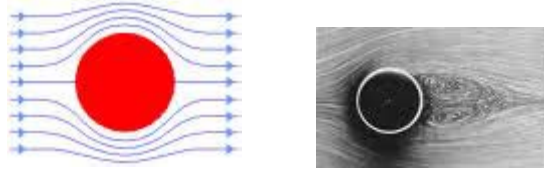


Figure 7: Flow patterns around a circular cylinder; (a) inviscid fluid [12]; and (b) viscous fluid [13].

COMPARING PRESSURE DISTRIBUTIONS IN INVISCID AND VISCOUS FLOWS

Looking at Figure 4 and Figure 5, it can be seen that at and near the leading edge, all measured pressure distributions are very close to those of an inviscid fluid. However, if one follows the fluid particle as it moves towards the trailing edge, the discrepancies between inviscid theory and the behaviour of real fluids become large. This is explained by the occurrence of flow separation and the subsequent formation of a viscous wake, Figure 7. In inviscid flow, fluid particles are accelerated while moving on the upstream half of the cylinder and decelerated on the downstream half of it. Since there is no dissipation of energy, pressure decreases on the upstream side are converted from pressure to kinetic energy there. The reverse occurs on the downstream side, which causes pressure to increase along the downstream half. The result is that the fluid particle stays on the surface of the cylinder at all times and leaves it with a speed equal to that which the same particle had when it first came in contact with the cylinder.

In real flows, however, viscosity is present, and a fluid particle that moves in the vicinity of the surface of the cylinder is within the viscous boundary layer, where, from boundary-layer theory, the pressure is the same as that existing outside the boundary layer [3][6][7]. Because this particle is subjected to a constant pressure, its decreases in kinetic energy during motion are not converted into pressure. Rather, they become losses created by frictional resistance. Therefore, when the particle enters the downstream half of the cylinder, its kinetic energy is smaller than it would have been in inviscid flow; and, somewhere along its path, it becomes unable to keep moving forward, stops, and external pressures force it to reverse directions. Reynolds numbers that are above critical values cause the boundary layer to become turbulent. The contribution of a turbulent boundary layer is that fluid particles within it have more linear momentum and kinetic energy than those in a laminar boundary layer under similar circumstances. Thus, turbulent boundary layers allow particles within it to travel farther along the contour of the cylinder and, are thus able to delay separation beyond the points where it would occur if the boundary layer had been laminar. This delayed separation increases pressure recovery, reduces the size of the viscous wake behind the cylinder and, ultimately, reduces total drag. This is why, for example, golf balls have dimples; dimples cause turbulence in the boundary layer [1].

CONCLUSIONS

Hands-on exercises were designed and tested in a subsonic wind tunnel to study pressure distributions around a circular cylinder in cross flow. They allowed students to use their own data to examine how the pressure on the surface of the cylinder changes with the location of a given point along the circumference of the middle cross-section of the cylinder and with the magnitude of the Reynolds number of the cross-flow. Results obtained were very similar to those in the research literature. Published data were used to augment the set of collected data beyond the maximum speed achieved by the wind tunnel. Results were used to demonstrate how viscous flow behaviour in the upstream half of the cylinder differed from that on its downstream half, and to examine how Reynolds numbers above the critical value that trips turbulence enhance the ability of a viscous flow to recover pressure on the downstream side of the cylinder and to reduce drag.

REFERENCES

1. Njock Libii, J., Dimples and drag: Experimental demonstration of the aerodynamics of golf balls, *American J. of Physics*, 75, 8, 764-767 (2007).
2. Vehicle Aerodynamic Factors (2009), 14 August 2010, www.kasravi.com
3. Batchelor, G.K., *An Introduction to Fluid Dynamics*. Cambridge: Cambridge University Press, 325-337, 364-365 (1994).
4. Flachsbart, O., Winddruck auf gasbehaelter. *Reports of the AVA in Goettingen*, 4th Series, 134-138 (1932).
5. Roshko, A., Experiments on the flow past a circular cylinder at very high Reynolds numbers. *J. of Fluid Mechanics*, 10, 345-356 (1961).
6. Debblor, W.R., *Fluid Mechanics Fundamentals*. Englewood Cliffs: Prentice Hall, 182 (1990).
7. Faber, T.E., *Fluid Dynamics for Physicists*. Cambridge: Cambridge University Press, 252-263 (1995).
8. Comparison of pressure variations in rectangular coordinates, 16 August 2010, http://www.ecourses.ou.edu/cgi-bin/ebook.cgi?doc=&topic=fl&chap_sec=07.4&page=theory
9. Douglas, J.F., Gasiorek, J.M. and Swaffield, J.A., *Fluid Mechanics*. Longman (1995).
10. Njock Libii, J., Laboratory exercises to study viscous boundary layers in the test section of an open-circuit wind tunnel. *World Transactions on Engng. and Technol. Educ.*, 8, 1, 91-97(2010).
11. Njock Libii, J., Design of an experiment to test the effect of dimples on the magnitude of the drag force on a golf ball. *World Transactions on Engng. and Technol. Educ.*, 5, 3, 477- 480 (2006).
12. Inviscid flow around a cylinder, 19 August, 2010, www.Altar.fiu.com
13. Viscous flow around a circular cylinder, 19 August, 2010, www.Knol.google.com